2-2-2018

Synthesis, Characterization, and In Vitro Cytotoxicity of Fatty Acyl-CGKRK-chitosan Oligosaccharides Conjugates for siRNA Delivery

Naglaa Salem El-Sayed
National Research Center, Egypt

Meenakshi Sharma
Chapman University

Hamidreza Montazeri Aliabadi
Chapman University, montazer@chapman.edu

Magda Goda El-Meligy
National Research Center, Egypt

Ahmed Kamed El-Zaity
Ain Shams University

See next page for additional authors

Recommended Citation

El-Sayed NS, Sharma M, Montazeri Aliabadi H, et al. Synthesis, characterization, and in vitro cytotoxicity of fatty acyl-CGKRK-chitosan oligosaccharides conjugates for siRNA delivery. *Int J Biol Macromol*. 2018;112:694-702. doi: 10.1016/j.ijbiomac.2018.01.213

Synthesis, Characterization, and In Vitro Cytotoxicity of Fatty Acyl-CGKRK-chitosan Oligosaccharides Conjugates for siRNA Delivery

Authors
Naglaa Salem El-Sayed, Meenakshi Sharma, Hamidreza Montazeri Aliabadi, Magda Goda El-Meligy, Ahmed Kamed El-Zaity, Zenat Adeeb Nageib, and Rakesh Tiwari

Accepted Manuscript

Synthesis, characterization, and in vitro cytotoxicity of fatty acyl-CGKRK-chitosan oligosaccharides conjugates for siRNA delivery

Naglaa Salem El-Sayed, Meenakshi Sharma, Hamidreza Montazeri Aliabadi, Magda Goda El-Meligy, Ahmed Kamed El-Zaity, Zenat Adeeb Nageib, Rakesh Kumar Tiwari

PII: S0141-8130(17)33216-6
DOI: https://doi.org/10.1016/j.ijbiomac.2018.01.213
Reference: BIOMAC 9045

To appear in:

Received date: 25 August 2017
Revised date: 18 January 2018
Accepted date: 31 January 2018

Please cite this article as: Naglaa Salem El-Sayed, Meenakshi Sharma, Hamidreza Montazeri Aliabadi, Magda Goda El-Meligy, Ahmed Kamed El-Zaity, Zenat Adeeb Nageib, Rakesh Kumar Tiwari , Synthesis, characterization, and in vitro cytotoxicity of fatty acyl-CGKRK-chitosan oligosaccharides conjugates for siRNA delivery. The address for the corresponding author was captured as affiliation for all authors. Please check if appropriate. Biomac(2017), https://doi.org/10.1016/j.ijbiomac.2018.01.213

Synthesis, characterization, and in vitro cytotoxicity of fatty acyl-CGKRK-chitosan oligosaccharides conjugates for siRNA delivery

Naglaa Salem El-Sayed[a,b], Meenakshi Sharma[b], Hamidreza Montazeri Aliabadi[b], Magda Goda El-Meligy[a], Ahmed Kamed El-Zaity[c], Zenat Adeeb Nageib[a], Rakesh Kumar Tiwari[b]*

[a]Cellulose and Paper Department, National Research Center, Dokki 12622, Cairo, Egypt

[b]Department of Biomedical and Pharmaceutical Sciences, Chapman University School of Pharmacy, Harry and Diane Rinker Health Science Campus, Irvine, CA 92618, United States

[c]Chemistry Department, Faculty of Science, Ain Shams University, Abbassia, Cairo 11566, Egypt

* Corresponding Author

Rakesh Kumar Tiwari, Ph. D.

Chapman University School of Pharmacy

Harry and Diane Rinker Health Science Campus

#263, 9401 Jeronimo Road

Irvine, CA 92618, USA

Tel: (714) 516-5483. Fax: (714) 516-5481. E-mail: tiwari@chapman.edu

Abstract:

In this studies, three fatty acyl derivatives of CGKRK homing peptides were coupled successfully to chitosan oligosaccharides (COS) using sulfosuccinimidyl-4-(*N*-maleimidomethyl)cyclohexane-1-carboxylate sodium salt (sulfo-SMCC). The COS-SMCC was prepared by direct coupling between COS and sulfo-SMCC in PBS (pH 7.5) at RT for 48 h. The structure of COS-SMCC and the three fatty acyl-CGKRK-SMCC-COS conjugates were characterized by FT-IR, ^{13}C NMR, and SEM. The ability of three conjugates to condense siRNA into nanosized polyplexes and their efficacy in protecting siRNA from serum nucleases degradation were investigated. Among the investigated derivatives, S-CGKRK-COS showed higher siRNA binding affinity as compared to the P-CGKRK-COS and O-CGKRK-COS respectively. At a ratio of 10:1, complete protection for siRNA from early enzymatic degradation was achieved. The polymers and the polymer/siRNA polyplexes showed negligible cytotoxicity on human breast cancer cell line MDA-MB-231 at all investigated ratios. However, the polyplexes prepared with palmitoyl and oleoyl derivatives at polymer concentration 10 µg/mL reduced the cell viability by 21.5% and 35% respectively. The results of this study revealed the impact of using fatty acyl-CGKRK-COS as a siRNA carrier and confirmed the importance of incorporating a hydrophobic moiety into chitosan to improve its capacity in complexing with siRNA and protection from degradation.

***Keywords*:** fatty acyl-CGKRK peptide, chitosan oligosaccharide, MDA-MB-231, siRNA delivery, cytotoxicity.

1. Introduction

The term gene therapy covers a wide range of treatments that employ the genetic material to modify cell activities. Gene therapy is the next generation strategy for fighting many heredity disorders, cancers, infectious, chronic, and neurodegenerative diseases [1]. So far, few approaches to gene therapies have been approved. The first gene therapy approved in the China was Gendicine in 2003 for the treatment of head and neck squamous cell carcinoma. Using Gendicine more than two thousands of patients have been treated alone in the China. Another example of the successful launch of gene therapy came in October 2012 in Europe where the European Medicines Agency (EMA) gave its permission to a gene therapy company UniQure at Amsterdam to approve Glybera, for the treatment of an extremely rare disease that inflames the pancreas. Similarly, EMA also approved GlaxoSmithKline together with Fondazione Telethon and Ospedale to launch Strimvelis, a pediatric gene therapy product that targets a rare immune disorder due to adenosine deaminase deficiency (ADA-SCID) [2].

Short interfering RNA (siRNA)-mediated gene silencing is an intracellular mechanism used for suppressing expression of certain proteins, leading to a phenotypical response. siRNA has demonstrated tremendous therapeutic potential for the treatment of many gene associated disorders and pathogens [3]. Over the years, several strategies for siRNA efficient delivery have been explored including polycationic liposomes, cationic polymers, nanoparticles, aptamers, cationic cell-penetrating peptides (CPPs), antibodies, and cationic lipids [4-9]. Despite the high gene transfection efficiency of viral carriers, the viral induced immunogenicity and the insertional mutagenesis are the major problems that impede their actual use on the clinical levels [3]. Due to the cytotoxicity profile, the high-cost effectiveness, and poor siRNA transfection efficiency for the non-viral carriers [10], there is a growing interest in developing successful

non-viral nucleic acid carriers that can address the safety, biocompatibility, biodegradability, and selectivity issues. With a great emphasis on their ability to stabilize their complexes with different forms of nucleic acid therapy, escape the phagocytosis, and protect its load from serum nucleases degradation [11].

Chitosan and its derivatives have inspired the investigators as a promising non-viral nucleic acid carrier because of their dense cationic nature, excellent biocompatibility, nearly negligible cytotoxicity and immune response. The high flexibility of chitosan backbone permits their further modifications to improve its transfection efficacy and selectivity [12, 13]. The potential of chitosan and its derivative as nucleic acid carrier is due to the primary amines along their backbone, which protonate in the acidic pH to positively charged amine groups that bind to the negatively charged DNA or siRNA via the electrostatic interaction, leading to the formation of nano-size complexes named polyplexes in the aqueous medium. Nevertheless, the limited siRNA transfection efficiency of chitosan and the lack of tissue selectivity, have inspired many researchers to look for solutions to surmount the aforementioned barriers and mediate siRNA transfection using chitosan derivatives.

Among the suggested approaches that have been investigated to overcome the *in vivo* limitations of siRNA delivery, is PEGylation of the carrier system. It has been found that the PEGylation of polycations can ameliorate the polycation toxicity, and prolong the *in vivo* half-life for the polyplexes. However, PEG affects the size, charge, stability of the formed polyplexes, and may hinder their cellular uptake. Therefore, a balance between PEGylation and de-PEGylation of the polyplexes is needed to enable the siRNA escape from the phagocytosis by the reticuloendothelial system and allow its proper uptake by the cells [12-15]. Furthermore, previous studies estimated the importance of incorporating a hydrophobic substituted to the

siRNA polymeric carrier. Since the hydrophobic fragment such as oleic acid, and stearic acid, or cholesterol significantly enhanced the siRNA cellular uptake, promoted its endosomal release into the cytoplasm, protected siRNA against serum nucleases digestion, and effectively improved the siRNA transfection efficacy [16-18].

Furthermore, a unique feature of the CPPs is their efficiency in transporting payloads into the target cell through active or passive mechanisms [19]. This feature has been employed to improve the chitosan transfection capacity and tissue selectivity through its conjugation to CPPs [20]. The attachment of targeting ligand to the drug and gene delivery systems has been found to be an effective strategy for achieving selective delivery of the chemotherapeutics to the tumor sites, due to the significant differentiation of the tumor tissue from the normal tissues [20, 21]. In 2011, L. Agemy *et al.* reported the success of the iron oxide nanoparticles decorated with CGKRK peptide in targeting glioblastoma, breast, and prostate cancer cell lines [22, 23]. The targeting by CGKRK peptide mediates the cellular internalization in energy and heparin sulfate receptor-dependent manners, which are overexpressed significantly in the cancer cells [22]. Recently, we have developed a library of fatty acyl CGKRK peptides, which were found to be potent in their ability to bind to siRNA, protect siRNA from the enzymatic degradation, and selectively target breast and prostate cancer cell lines and induced siRNA silencing for kinesin spindle protein (KSP) [24]. The results indicated that the stearic/oleic acid-peptide conjugates showed the highest efficiency in siRNA uptake and silencing of kinesin spindle protein (KSP) at a peptide: siRNA ratio of 80:1. Therefore, we decided to explore the impact of conjugating chitosan oligosaccharide to the palmitoyl, stearoyl, and oleoyl CGKRK peptide and evaluate the efficiency of the delivery system in the formation of a complex with siRNA and protecting it from serum nucleases degradation and dissociation by other competing species such as heparin.

2. Materials and methods

2.1. Materials

Chitosan oligosaccharides (COS) MW = 4000-5000 Da, with 90% degree of deacetylation, palmitic, stearic acid, or oleic acid and 3-[4,5-Dimethylthiazol-2-yl]-2,5-diphenyl tetrazolium bromide (MTT), heparin sulfate were purchased from Sigma-Aldrich Chemical Co. (Milwaukee, WI, USA). For the synthesis of fatty acyl-CGKRK peptides, all required organic solvents were purchased from Wilkem Scientific (Pawtucket, RI, USA). Coupling reagents include Rink amide MBHA resin, and Fmoc-amino acid building blocks were purchased from Chem-Impex International Inc. (Wood Dale, IL, USA). Other reagents and chemicals were purchased from Sigma-Aldrich Chemical Co. (Milwaukee, WI, USA).

Hanks Balanced Salt Solution (HBSS), Dulbecco's modified Eagle medium (DMEM; low glucose with L-glutamine), RPMI Medium 1640 with L-glutamine, Fetal bovine serum (FBS), SYBR Green II, penicillin (10000 U/mL), and streptomycin (10 mg/mL) were provided by Life Technologies (Grand Island, NY, USA). Scrambled negative control siRNA (Catalogue # AM4635), 5′-carboxyfluorescein (FAM)-labeled negative control siRNA (Catalogue # AM4620), and the siRNA targeting kinesin spindle protein (KSP; Catalogue # AM16704) were obtained from Ambion (Austin, TX) SYBR Green Supermix were supplied by Bio-Rad (Hercules, CA). Ethylenediamine tetraacetic acid (EDTA) and all other materials were obtained from Fisher Scientific (Carlsbad, CA). Human breast cancer cell line MDA-MB-231 (ATCC #HTB-26) was purchased from American Type Culture Collection (ATCC; Manassas, VA). MDA-MB-231 was cultured in DMEM medium. Media were supplemented with 10% (v/v) fetal bovine serum, 100 U/mL penicillin and 100 μg/ml streptomycin. Cells were maintained in the

normal condition of 37 °C and 5% CO_2 under humidified atmosphere and were sub-cultured when 80-100% confluent.

2.2. Synthesis of fatty acyl-CGKRK peptides

In general, the CGKRK peptide was synthesized using solid-phase synthesis strategy employing *N*-(9-fluorenyl)methoxy-carbonyl (Fmoc)-based peptide chemistry. Fmoc-L-amino acids were used as building blocks. The CGKRK peptide sequence was synthesized on Tribute automated peptide synthesizer (Protein Technology, Inc., Arizona) in 0.40 mmol scale. The fatty acylation was performed on a solid support using palmitic acid, stearic acid, and oleic acid. HTBU and DIPEA were used as coupling reagents as reported [24]. The mass of synthesized peptide was fully characterized using high-resolution matrix-assisted laser desorption−ionization time-of-flight (MALDI-TOF/TOF) mass spectrometer (ABX SCIEX TOF/TOF) and lyophilized before using to conjugate chitosan.

2.3. Synthesis of COS-SMCC

The coupling of COS to sulfo-SMCC was carried out as reported [25]. The resulted COS-SMCC was purified using dialysis tube (MWCO 1000 Da) against distilled water for 3 days and freeze-dried affording COS-SMCC as a powder.

2.4. Synthesis of fatty acyl-CGKRK-COS

In brief, 50 mg of COS-SMCC was dissolved in 10 mL of phosphate buffer solution at pH 6.5 and stirred for 30 min. Then, the solution of a fatty acyl-CGKRK peptide (2 mM) in PBS with pH 6.5 was added dropwise over 30 min. The conjugation reaction was continued under stirring for an additional 48 h at room temperature in the dark. The resulting fatty acyl-CGKRK-

COS conjugates were purified using dialysis tube with MWCO 1000 Da for three days against MilliQ-water. Then, the dialyzed polymers were freeze-dried to obtain the corresponding fatty acyl-CGKRK-COS powder for further biological assays.

2.5. FT-IR

FT-IR spectra for COS, COS-SMCC, and fatty acyl-CGKRK-COS were obtained with (Alpha FT-IR Spectrometer/Platinum ATR) from Bruker.

2.6. ^{13}C NMR

^{13}C NMR spectra for COS, COS-SMCC, and fatty acyl-CGKRK-COS were recorded on a Bruker Avance III HDTM 400 NMR spectrometer in D_2O. Chemical shifts are shown in parts per million (ppm).

2.7. Scanning electron microscopy (SEM)

The samples of COS, COS-SMCC, and fatty acyl-CGKRK-COS were imaged with a SEM Phillips XL-30 scanning electron microscope, UCI, California, USA, by sprinkling onto an aluminum stub covered with copper tape.

2.8. Preparation of polymer/siRNA nano polyplexes

The polymer/siRNA polyplexes were prepared in 0.15 M NaCl with stock polymer (1 mg/mL) and scrambled siRNA (0.14 µg/µL) solutions. For complex formation, a solution of scrambled siRNA was mixed with the polymer solution at ratios (1:1, 2.5:1, 5:1, and 10:1; w/w).

Then they were subjected to gentle vortex for 30 sec and incubated at room temperature for 30 min before use or further experiments.

2.9. Dynamic light scattering measurements

Particle size and zeta potential of the different formulations at different polymer:siRNA ratio were determined following a dynamic light scattering (DLS) method using Malvern Zeta Sizer (Nano ZS; Malvern, Instruments, UK) equipped with photodiode detector at 90° orientation. The nano polyplex were freshly prepared as mentioned in section 2.8, then the volume of each sample was completed to 1 mL by adding a saline solution. Then the size and zeta potential of the complexes were measured in triplicate at 25 ºC.

2.10. SYBR green dye exclusion assay

The affinity of the polymers to bind to the siRNA was assessed by the SYBR Green II binding assay. Briefly, scrambled siRNA solutions (1.25 µL /100 µL) were prepared in 0.15 M NaCl (in duplicate) and the polymer solution (1 mg/mL) was added to the siRNA solution in different volumes to create different polymer:siRNA weight ratios from 0.2:1, 0.4:1, 0.8:1, 1.6:1, 2.4:1, 3.2:1, and 6.4:1. After 30 min incubation at room temperature, 200 µL of the SYBR Green II solution was added to the complexes, and the fluorescence of the samples was measured in a 384 well plate (ex: 485 nm, em: 527 nm) to quantify the amount of free siRNA. The binding curves were generated by plotting the percentage of siRNA bound to the polymer vs. polymer to siRNA ratio as described above, and the BC_{50} value was calculated based on the ratio that yielded 50% binding under the experimental conditions.

2.11. Serum stability and heparin dissociation assays

Samples of unprotected (naked) scrambled siRNA, and polymer/siRNA nano polyplexes were prepared with polymer:siRNA ratios of (2.5:1, 5:1, 7.5:1, and 10:1; Wt/Wt). The polyplexes were incubated in triplicates at 37 ^{o}C in triplicate with 25% v/v fetal bovine serum (FBS) solution in HBSS for 24 h (FBS) for 24 h. At the end of incubation period, 2 µL of 5% heparin solution in saline and 3 µL of 0.5 mM EDTA solution were added to the samples and incubated at 37 ^{o}C for 1 h to ensure complete dissociation of remaining siRNA from the polymers. Samples were then analyzed for the remaining intact siRNA by agarose gel electrophoresis using 1% agarose gel containing 1 µg/mL ethidium bromide (EtBr) at 70 V for 20 min. The gel was visualized under UV illumination (Gel-Doc system, Bio-Rad; Hercules, CA), and the intensity of the bands corresponding to the remaining intact siRNA was quantified using Image J software, and digitalized pictures were analyzed with Scion Image analysis software to determine the siRNA band density.

2.12. Cytotoxicity of the polymer and the polymer/siRNA polyplexes

Polymer/siRNA complexes were prepared using the scrambled siRNA at the ratio of 8:1 and added to the wells to give final polymer concentrations of 1.25, 2.5, 5, and 10 µg/ mL in triplicate. Then, the cells were incubated for 48 h in their normal maintenance conditions, and then 40 µL of MTT solution (5 µg/ mL in HBSS) was added to each well. After 2 h of incubation in 37 ^{o}C, the medium was removed, and 500 µL of DMSO was added to each well to dissolve the formed crystals. The optical density of the wells was measured with UV-2600 (UV-Vis Spectrophotometer, Shimadzu, USA) with the cell-less medium as a blank. The absorbance of

polymer treated cells was compared to untreated cells (as 100% viability), and the percent of cell viability was calculated for each concentration of polymers.

3. Results and Discussion

The success of CGKRK peptide in achieving selective delivery of many biologically active molecules such as anticancer drugs and siRNA to the tumor tissues [22-24, 26] promoted our research group to explore the potential efficacy of this short peptide in different formulations to target siRNA to different cancer cells. Recently, we have developed a library of fatty acyl (Fa) CGKRK peptides which were found potent in their ability to bind to siRNA. The palmitoyl-CGKRK (P-CGKRK), stearoyl-CGKRK (S-CGKRK), and oleoyl-CGKRK (O-CGKRK) peptides showed promising efficacy in mediate siRNA transfection, gene silencing, and *in vitro* tumor selectivity when investigated on prostate, breast cancer cell lines, and healthy kidney cell line [24]. Therefore, we selected these three Fa-CGKRK derivatives and coupled them to COS to investigate the impact of using COS in forming complexes with siRNA and its ability in the protection of siRNA from serum RNas.

In this study, the water soluble and reactive COS with the average molecular weight 4000-5000 Da, and degree of deacetylation 90% was used as a carrier for siRNA. However, the lack of selectivity, limited cellular uptake and transfection efficacy of COS encouraged us to modify COS by coupling three different fatty acyl-CGKRK peptides via a sulfo-SMCC bifunctional linker (Scheme 1).

3.1. Coupling of COS to fatty acyl-CGKRK

The strategy first involved the immobilization of the bifunctional linker (sulfo-SMCC) on the surface of the water-soluble COS as described by us to form COS-SMCC [21]. Three fatty acyl-CGKRK peptides namely, P-CGKRK, S-CGKRK, and O-CGKRK were synthesized and characterized as reported by us. [24]. Then, Fa-CGKRK peptides were coupled through the formation of stable thioether bond between the peptide reduced sulfhydryl groups and the maleimide arm of COS-SMCC (Scheme 1). The structures of the new conjugates were confirmed by FT-IR, ^{13}C NMR, and SEM.

3.2. Characterization for fatty acyl-CGKRK-COS

3.2.1. FT-IR of the conjugates:

FT-IR spectra for COS, COS-SMCC, and fatty acyl-CGKRK-COS confirm the functional groups after covalent coupling in the conjugated polymer. As shown in Fig. 1, the FT-IR of COS revealed the presence of the following absorption bands at 3240 cm^{-1}, 2921 cm^{-1}, 1673 cm^{-1}, and 1550 cm^{-1} which were due to the stretching vibrational bands of –NH_2, C–H aliphatic, C=O acetyl, and the bending vibrational band of N–H respectively. For COS-SMCC, the shift in the stretching vibrational bands from 1673 cm^{-1} to 1668 cm^{-1} and the appearance of strong sharp absorption band at 1626 cm^{-1} corresponds to the acetyl C=O and the NH-C=O amide I and II due to the conjugation between COS, and SMCC. In addition to the bending vibrational band at 1531 cm^{-1} for N–H group and the two stretching vibrational bands at 1093 cm^{-1} and 1053 cm^{-1} which was assigned to the different etheric C-O-C bonds. The peak at 674 cm^{-1} revealed the presence of the bending maleimide (C-H) band [21, 25, 27]. The coupling of the fatty acyl-CGKRK peptides to COS-SMCC was evidenced by the increased intensity of the stretching vibrational bands at

2918-2853 cm^{-1} due to the stretching band for aliphatic C–H of the fatty acyl side chains and the amino acids side chain. The absorption bands at 1683 cm^{-1}, 1633 cm^{-1}, 1672 cm^{-1}, 1638 cm^{-1}, 1671 cm^{-1}, 1625 cm^{-1} were assigned to the symmetric stretching bands of C=O amide bonds and C=O acetyl groups for the palmitoyl, stearoyl, and oleoyl COS derivatives. While the bending N–H of the deacetylated amine along the chitosan backbone of the three polymer conjugates appeared at 1526 cm^{-1}, 1526 cm^{-1}, and 1523 cm^{-1} respectively.

3.2.2. Structure characterization of conjugates using ^{13}C NMR spectroscopy

Figure 2 depicts the ^{13}C NMR spectrum for starting material and conjugated compounds such as COS, COS-SMCC, and fatty acyl-CGKRK-COS which showed a characteristic peak for the structural confirmation of the conjugated compounds. The spectra of COS (D_2O) in fig 2a revealed the existence of the following signals at δ (ppm) values of 22.08 for CH_3 (acetyl), 66.60 - 101.34 were assigned to carbon atoms C6, C5, C4, C3, C2 and C1 of the anhydroglucose amine units, and a single peak for CO (acetyl carbonyl) at 181.87 ppm [26]. The successful conjugation of SMCC linker to the COS chain was revealed in fig 2b, where the characteristic peaks in the region of 26.98 - 101.17 ppm were attributed to the SMCC linker, (C1-C6) of chitosan anhydroglucose amine units. The distinctive signal of maleimide arm (HC=CH) appeared at δ value of 131.58 ppm [25]. While the signals at δ values in 165.32, 174.75, and 179.01 ppm were assigned to the three different CO (amidic carbonyl) and one CO (acetyl carbonyl) groups of COS-SMCC chains [21]. The coupling of fatty acyl-CGKRK peptides to COS-SMCC were confirmed by analyzing the ^{13}C NMR spectra (fig 2c-2e) which revealed the appearance of a new signal at δ (ppm) values at 16.57, 16.54, and 13.96 ppm for the terminal CH_3 of the palmitoyl, stearoyl, and oleoyl chains respectively. Furthermore, the signals at the region 156-178 ppm in

fig 2c-d were attributed to the carbonyl groups of CGKRK peptide, chitosan backbone, and those of SMCC linker. Additionally, the clear signal in the ^{13}C-NMR spectrum of O-CGKRK-COS at δ value of 131.20 ppm was assigned to the oleoyl ethylenic group (CH=CH) [28]. These ^{13}C-NMR assignments for COS-fatty acyl peptide conjugates were in agreement with the reported data in the literature.

3.2.3. Characterization of the copolymer morphology by SEM

The morphology of COS, COS-SMCC, and the three derivatives of fatty acyl-CGKRK-COS conjugates were examined and compared to unmodified COS and COS-SMCC by the scanning electron microscopy. As shown in Fig. **3a-e**, the sequential functionalization of COS with SMCC, and fatty acyl-CGKRK changed the morphology of COS from granulated particles to fibrous, network like structures with several large pores size.

3.3. Size and zeta potential analysis

The hydrodynamic size for the polymer/siRNA complexes at different weight ratios of the polymers to siRNA was determined as reflected in fig 4a. Overall the hydrodynamic particles size varied by varying the polymer ratio, and the hydrophobic moiety conjugated to the CGKRK peptide. At ratio 5:1, the polyplexes had particle size ranged from 204-386 nm, and the smallest particle size achieved by O-CGKRK-COS. As the polymer: siRNA ratio increase from 5:1 to 10:1, the two conjugated polymers (P-CGKRK-COS and O-CGKRK-COS) exhibited decrease in the hydrodynamic diameter. Meanwhile, S-CGKRK-COS polymer showed increase in hydrodynamic diameter (204-274nm). Interesting, S-CGKRK-COS polymer at polymer: siRNA ratio of 1:1 showed highest diameter at this ratio as compared to other two polymers.

Furthermore, the conjugation of COS to the fatty acyl-CGKRK peptide efficiently improved the complexing ability with siRNA and potentially reduced the hydrodynamic size to less than 200 nm at a ratio of 10:1 in comparison to the fatty acyl-CGKRK alone which gave nanoplexes with hydrodynamic size 300-400 nm at peptide: siRNA ratio of 10: 1 [24] (Fig.4a).

The values obtained from zeta potential measurement showed that fatty acyl-CGKRK-COS polymers had higher zeta potential compared to unmodified COS at the same ratio of polymer: siRNA. The increase in the zeta potential in the functionalized polymer can be attributed to the increase in average molecular weight of the Fa-CGKRK-COS and the cationic nature of the coupled peptide which has two lysine and one arginine moieties. For all Fa-CGKRK-COS derivatives, a continuous increase in the zeta-potential was observed with increasing the polymer:siRNA ratio. All polymers showed positive zeta potential at the ratio of 5:1 and started to plateau at ratio 10:1, except COS, which had a positive value of 4.3 mv at a ratio of 10:1. The data revealed that the oleoyl substitution effectively shifted the zeta potential to more positive values compared to the palmitoyl and the stearoyl derivatives which indicates its strong ability in assembling with siRNA (Fig. 4b).

3.4. Binding affinity of the polymers to siRNA

The affinity of each polymer to form complexes with siRNA was determined by SYBR green test. The SYBR green dye tends to bind to the uncomplexed (free) siRNA Fig. 5a. The results showed that COS had the highest affinity to complex with siRNA compared to the other investigated three derivatives of fatty acyl peptide –COS, and this trend was expected due to the hydrophilic nature of COS. The binding affinity for the three COS derivatives with increasing

ratio were in the following order: unmodified COS > S-CGKRK-COS ≈ O-CGKRK-COS ≈ P-CGKRK-COS.

The ratio of polymer: siRNA at which 50% of siRNA binding was achieved, is defined as BC_{50} which was calculated for each polymer from the binding affinity curves. BC_{50} correlates the degree of polymer hydrophobicity to the binding affinity of siRNA. Fig. 5b showed a correlation between BC_{50} and the number of carbon atoms of the attached fatty acid. It can be concluded that the BC_{50} decreases as in such order: COS < O-CGKRK-COS ≈ S-CGKRK-COS < P-CGKRK-COS. The calculated BC_{50} for S-CGKRK-COS and O-CGKRK-COS were almost the same and less than the palmitoyl derivative.

3.5. Serum stability test of nano polyplexes

The carrier system should be able to protect siRNA from degradation by serum RNAase A-type nucleases which play a critical role in reducing the circulation half-life of siRNA to less than 30 min [27]. The polymer/siRNA complexes were prepared at different weight ratios (2.5, 5, 7.5, and 10) and incubated in triplicate with 25% FBS solution in HBSS (v/v) for 24 h at 37 ^{o}C, then the percentage of intact siRNA was determined by agarose gel electrophoresis (Fig. 6). A regular trend in the increase of siRNA protection from serum lytic enzymes was achieved at polymer: siRNA ratios of 2.5:1, 5.0:1, 7.5:1, and 10:1 for all the polymers whereas S-CGKRK-COS showed a minor increase in protection during increase in ratios from 7.5:1 to 10:1. The impact of fatty acid conjugation to CGKRK was studied in our previous studies [24], which indicated that the attachment of fatty acyl moiety to CGKRK peptide improved its ability to protect siRNA from serum RNAas degradation. Although, fatty acyl CGKRK had negligible to limited abilities in protecting siRNA (0% to less than 55%) at peptide:siRNA w/w ratios of 5:1

(N/P ≈ 6.8), and 10:1 (N/P ≈ 13.6), however all the conjugates, e.g., Fa-CGKRK-COS achieved different degrees of protection for siRNA. Our experiments revealed that degree of serum degradation was dependent on the polymer ratio and its degree of hydrophobicity. Generally, increasing the polymer ratio increased its ability to protect siRNA from serum degradation. Where COS protected 98.7% of siRNA at polymer ratio 10. Meanwhile, the palmitoyl, oleoyl, and stearoyl derivatives protected about 91.6, 94.7 and 98% of siRNA at the same polymer ratios. In conclusion, the conjugation of COS to the fatty acyl peptides exerted a positive effect in stabilizing and protecting siRNA from degradation the fatty acyl peptide to siRNA.

3.6 Evaluation of cytotoxicity of the polymer and polymer/siRNA polyplexes

The cytotoxicity of COS, fatty acyl-CGKRK-COS alone, and fatty acyl-CGKRK-COS/siRNA polyplexes were assessed on human breast cancer cell line MDA-MB-231 using MTT assay. The test was carried out at polymer concentrations of 1.25, 2.5, 5, and 10 µg/mL. All polymers showed a safer toxicity profile at 1.25 µg/ml, however at the highest concentration used 10 µg/ml, COS, and O-CGKRK-COS derivative exhibited a mild toxicity by 25% and 14% respectively. The toxicity of COS increase by increasing its concentration. Meanwhile, the cytotoxicity of both P-CGKRK-COS and S-CGKRK-COS were almost negligible at all investigated concentrations, as shown in Fig. 7a. Regarding the cytotoxicity of polymers/siRNA complexes, a negligible cytotoxicity was observed for the polyplexes at all investigated ratios except for the polyplexes prepared with palmitoyl and oleoyl derivatives which displayed a mild toxicity profile by 35.6% and 21.5% at the polymer/siRNA ratio of 10:1 respectively (Fig. 7b).

4. Conclusions

Using sulfo-SMCC linker, we have successfully immobilized fatty acyl-CGKRK peptide motif on the surface of chitosan oligosaccharide aiming to improve the efficacy of fatty acyl-CGKRK as a siRNA carrier system. The structure of the new polymers constructs were elucidated by FT-IR, ^{13}C NMR, and SEM. The new Fa-CGKRK-COS derivatives displayed improved siRNA binding affinities. The results suggested that Fa-CGKRK-COS conjugates were able to protect siRNA from the degradation by the serum lytic enzymes, particularly at high polymer ratio better than COS and Fa-CGKRK peptides alone. Additionally, the polyplexes with siRNA did not exhibit significant cytotoxicity even at the high polymer concentrations. It could be concluded that O-CGKRK-COS is promising carrier system for selective delivery of siRNA to the multi-drugs resistant breast cancer cell line. The ability of O-CGKRK-COS to mediated selective siRNA transfection in MDA-231 will be studied in future work.

Acknowledgements

The authors greatly acknowledge financial support for this research from Chapman University School of Pharmacy and Egyptian Cultural Affairs and Mission Sector, Ministry of Higher Education, Egypt.

Conflict of interest

The authors declare that they do not have competing or conflicting interests.

References

[1] D. Ibraheem, A. Elaissari, H. Fessi, Gene therapy and DNA delivery systems, Int. J. Pharm. 459 (2014) 70-83.

[2] S.L. Ginn, I.E. Alexander, M.L. Edelstein, M.R. Abedi, J. Wixon, Gene therapy clinical trials worldwide to 2012 - an update, J. Gene Med. 15 (2013) 65-77.

[3] J. Wang, Z. Lu, M.G. Wientjes, J.L. Au, Delivery of siRNA therapeutics: barriers and carriers, AAPS J. 12 (2010) 492-503.

[4] H. Lv, S. Zhang, B. Wang, S. Cui, J. Yan, Toxicity of cationic lipids and cationic polymers in gene delivery, J. Control. Release 114 (2006) 100-109.

[5] M. Morille, C. Passirani, A. Vonarbourg, A. Clavreul, J.P. Benoit, Progress in developing cationic vectors for non-viral systemic gene therapy against cancer, Biomaterials 29 (2008) 3477-3496.

[6] T. Endoh, T. Ohtsuki, Cellular siRNA delivery using cell-penetrating peptides modified for endosomal escape, Adv. Drug Deliv. Rev. 61 (2009) 704-709.

[7] C.E. Thomas, A. Ehrhardt, M.A. Kay, Progress and problems with the use of viral vectors for gene therapy, Nat. Rev. Genet. 4 (2003) 346-358.

[8] V. Bagalkot, X. Gao, siRNA-aptamer chimeras on nanoparticles: preserving targeting functionality for effective gene silencing, ACS Nano 5 (2011) 8131-8139.

[9] J. Zhou, K.T. Shum, J.C. Burnett, J.J. Rossi, Nanoparticle-Based Delivery of RNAi Therapeutics: Progress and Challenges, Pharmaceuticals (Basel) 6 (2013) 85-107.

[10] T. Niidome, L. Huang, Gene therapy progress and prospects: nonviral vectors, Gene Ther. 9 (2002) 1647-1652.

[11] D.W. Pack, A.S. Hoffman, S. Pun, P.S. Stayton, Design and development of polymers for gene delivery, Nat. Rev. Drug Discov. 4 (2005) 581-593.

[12] S.P. Strand, S. Lelu, N.K. Reitan, C. de Lange Davies, P. Artursson, K.M. Varum, Molecular design of chitosan gene delivery systems with an optimized balance between polyplex stability and polyplex unpacking, Biomaterials 31 (2010) 975-987.

[13] J. Malmo, H. Sorgard, K.M. Varum, S.P. Strand, siRNA delivery with chitosan nanoparticles: Molecular properties favoring efficient gene silencing, J. Control. Release 158 (2012) 261-268.

[14] T.H. Kim, H.L. Jiang, D. Jere, I.K. Park, M.H. Cho, J.W. Nah, Y.J. Choi, T. Akaike, C.S. Cho, Chemical modification of chitosan as a gene carrier in vitro and in vivo, Prog. Polym. Sci. 32 (2007) 726-753.

[15] M. Malhotra, C. Tomaro-Duchesneau, S. Saha, S. Prakash, Intranasal, siRNA Delivery to the Brain by TAT/MGF Tagged PEGylated Chitosan Nanoparticles, J Pharm (Cairo) 2013 (2013) 812387.

[16] Z.H. Liu, Z.Y. Zhang, C.R. Zhou, Y.P. Jiao, Hydrophobic modifications of cationic polymers for gene delivery, Prog. Polym. Sci. 35 (2010) 1144-1162.

[17] B.Q. Wang, C.B. He, C. Tang, C.H. Yin, Effects of hydrophobic and hydrophilic modifications on gene delivery of amphiphilic chitosan based nanocarriers, Biomaterials 32 (2011) 4630-4638.

[18] B. Layek, M.K. Haldar, G. Sharma, L. Lipp, S. Mallik, J. Singh, Hexanoic Acid and Polyethylene Glycol Double Grafted Amphiphilic Chitosan for Enhanced Gene Delivery: Influence of Hydrophobic and Hydrophilic Substitution Degree, Mol. Pharm. 11 (2014) 982-994.

[19] B. Layek, L. Lipp, J. Singh, Cell Penetrating Peptide Conjugated Chitosan for Enhanced Delivery of Nucleic Acid, Int. J. Mol. Sci. 16 (2015) 28912-28930.

[20] S.M. Weis, D.A. Cheresh, Tumor angiogenesis: molecular pathways and therapeutic targets, Nat. Med. 17 (2011) 1359-1370.

[21] N.S. El-Sayed, A.N. Shirazi, M.G. El-Meligy, A.K. El-Ziaty, Z.A. Nagieb, K. Parang, R.K. Tiwari, Design, synthesis, and evaluation of chitosan conjugated GGRGDSK peptides as a cancer cell-targeting molecular transporter, Int. J. Biol. Macromol. 87 (2016) 611-622.

[22] L. Agemy, D. Friedmann-Morvinski, V.R. Kotamraju, L. Roth, K.N. Sugahara, O.M. Girard, R.F. Mattrey, I.M. Verma, E. Ruoslahti, Targeted nanoparticle enhanced proapoptotic peptide as potential therapy for glioblastoma, Proc. Natl. Acad. Sci. U. S. A. 108 (2011) 17450-17455.

[23] E. Ruoslahti, Peptides as Targeting Elements and Tissue Penetration Devices for Nanoparticles, Adv. Mater. 24 (2012) 3747-3756.

[24] M. Sharma, N.S. El-Sayed, H. Do, K. Parang, R.K. Tiwari, H.M. Aliabadi, Tumor-targeted delivery of siRNA using fatty acyl-CGKRK peptide conjugates, Sci. Rep. 7 (2017) 6093.

[25] X. Nie, J.K. Zhang, Q. Xu, X.G. Liu, Y.P. Li, Y. Wu, C.Y. Chen, Targeting peptide iRGD-conjugated amphiphilic chitosan-co-PLA/DPPE drug delivery system for enhanced tumor therapy, J. Mater. Chem. B 2 (2014) 3232-3242.

[26] M. Rinaudo, Chitin and chitosan: Properties and applications, Prog. Polym. Sci. 31 (2006) 603-632.

[27] C.Y. Yan, J.W. Gu, D.P. Hou, H.Y. Jing, J. Wang, Y.Z. Guo, H. Katsumi, T. Sakane, A. Yamamoto, Synthesis of Tat tagged and folate modified N-succinyl-chitosan self-assembly nanoparticles as a novel gene vector, Int. J. Biol. Macromol. 72 (2015) 751-756.

Captions

Scheme 1: The synthesis of conjugated fatty acyl-CGKRK-COS.

Figures Legends:

Fig. 1: FT-IR for (a) COS, (b) COS-SMCC, (c) P-CGKRK-COS, (d) S-CGKRK-COS, and (e) O-CGKRK-COS.

Fig. 2: ^{13}C NMR (D_2O) for (a) COS, (b) COS-SMCC, (c) P-CGKRK-COS, (d) S-CGKRK-COS, and (e) O-CGKRK-COS.

Fig. 3: SEM of (a) COS, (b) COS-SMCC, (c) P-CGKRK-COS, (d) S-CGKRK-COS, and (e) O-CGKRK-COS.

Fig. 4: (a) The polymer/siRNA complexes hydrodynamic size; (b) The zeta potential of polymer/siRNA complex.

Fig. 5: (a) Binding affinity of the copolymers to scrambled siRNA; (b) The correlation between the length of the fatty acid conjugate and the polymer: scrambled siRNA ratio required for 50% binding.

Fig. 6: The serum stability of polymer/siRNA complex.

Fig. 7: **(**a) The cytotoxicity of COS, P-CGKRK-COS, S-CGKRK-COS, and O-CGKRK-COS without siRNA; (b) The cytotoxicity of COS/siRNA, S-CGKRK-COS/siRNA, P-CGKRK-COS/siRNA, and O-CGKRK-COS/siRNA complexes.

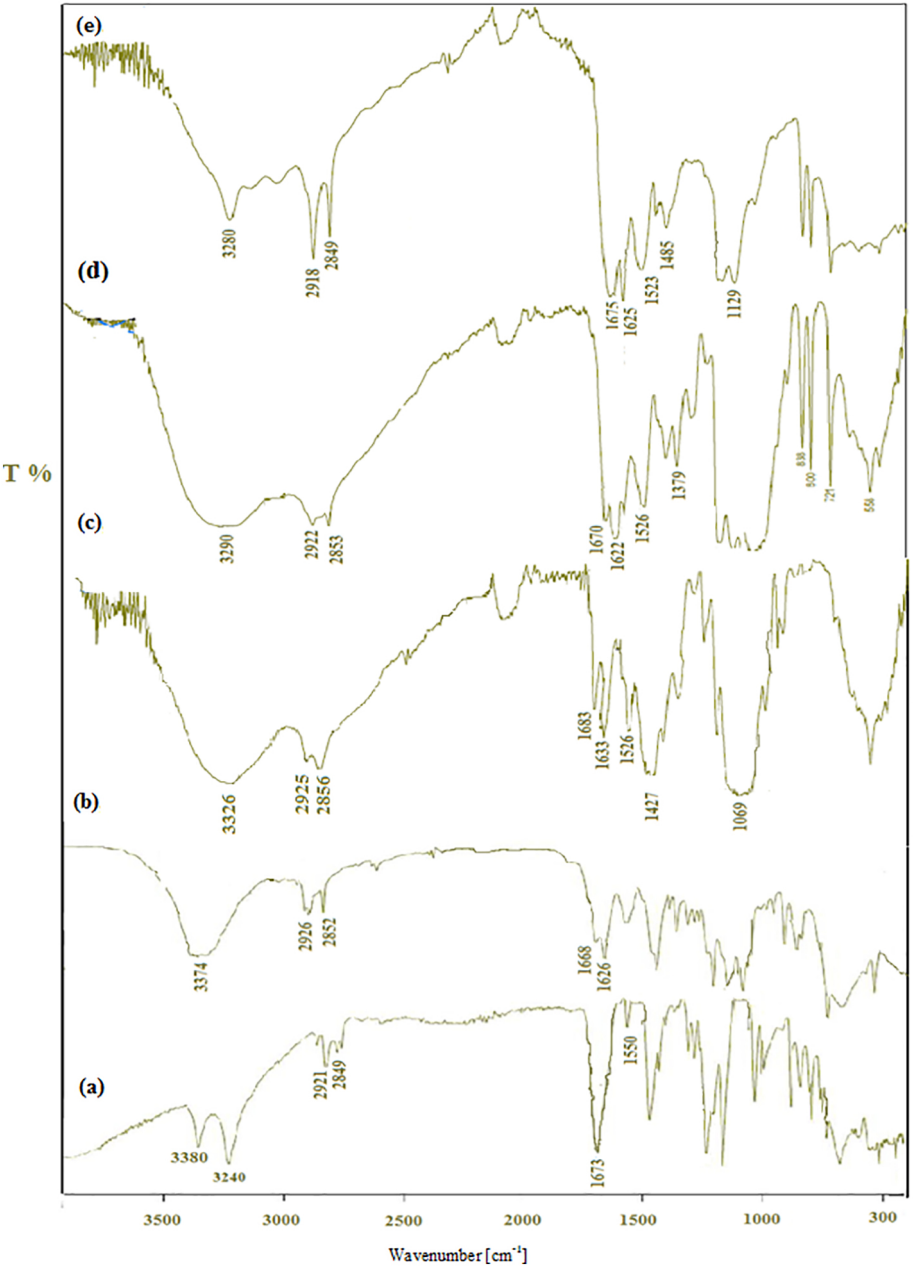
(e)
3280
2918
2849
1675
1625
1523
1485
1129
(d)
3290
2922
2853
1670
1622
1526
1379
838
550
721
550
(c)
3326
2925
2856
1683
1633
1526
1427
1069
(b)
3374
2926
2852
1668
1626
(a)
3380
3240
2921
2849
1673
1550
T %
3500
3000
2500
2000
1500
1000
300
Wavenumber [cm-1]

Figure 1

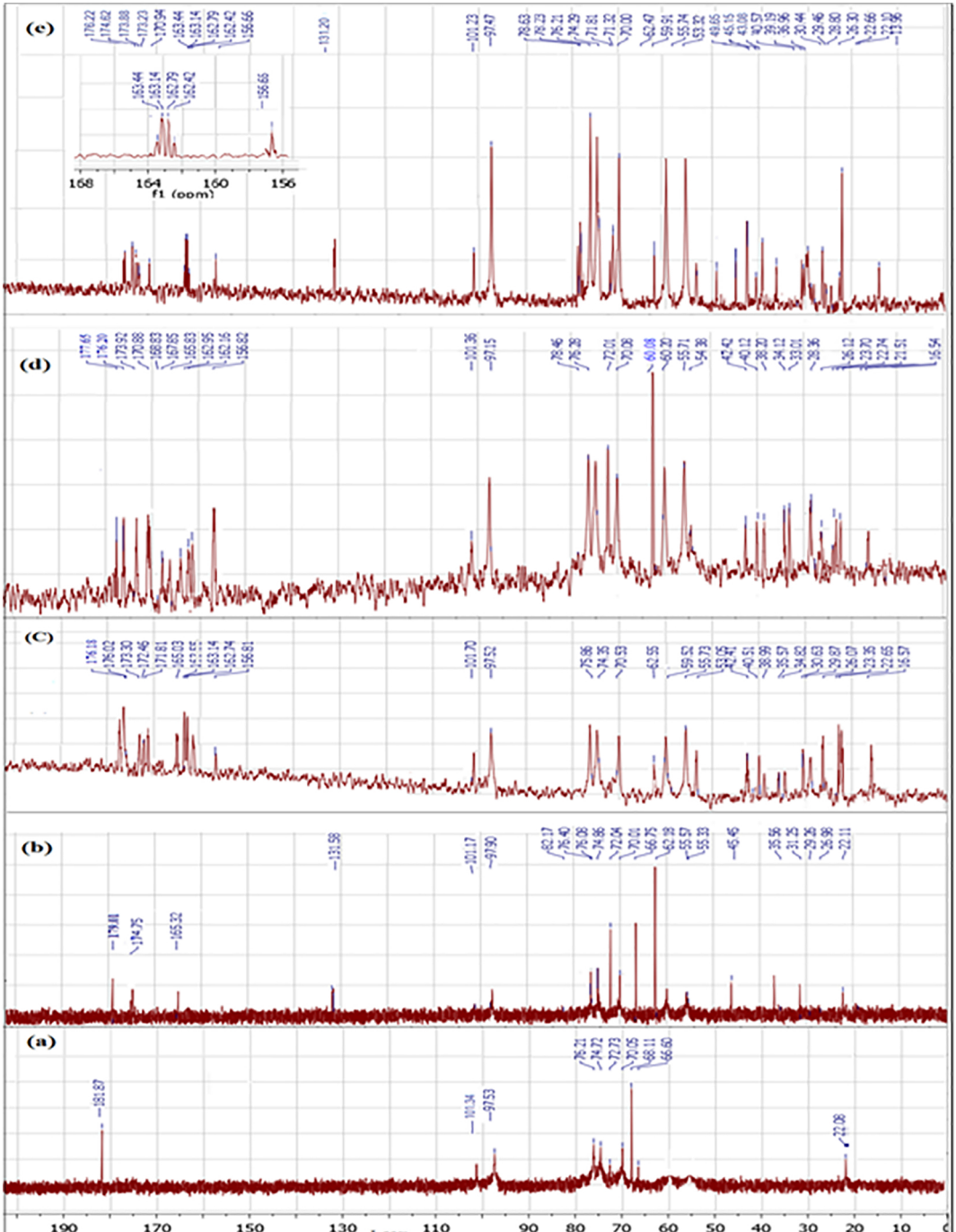

Figure 2

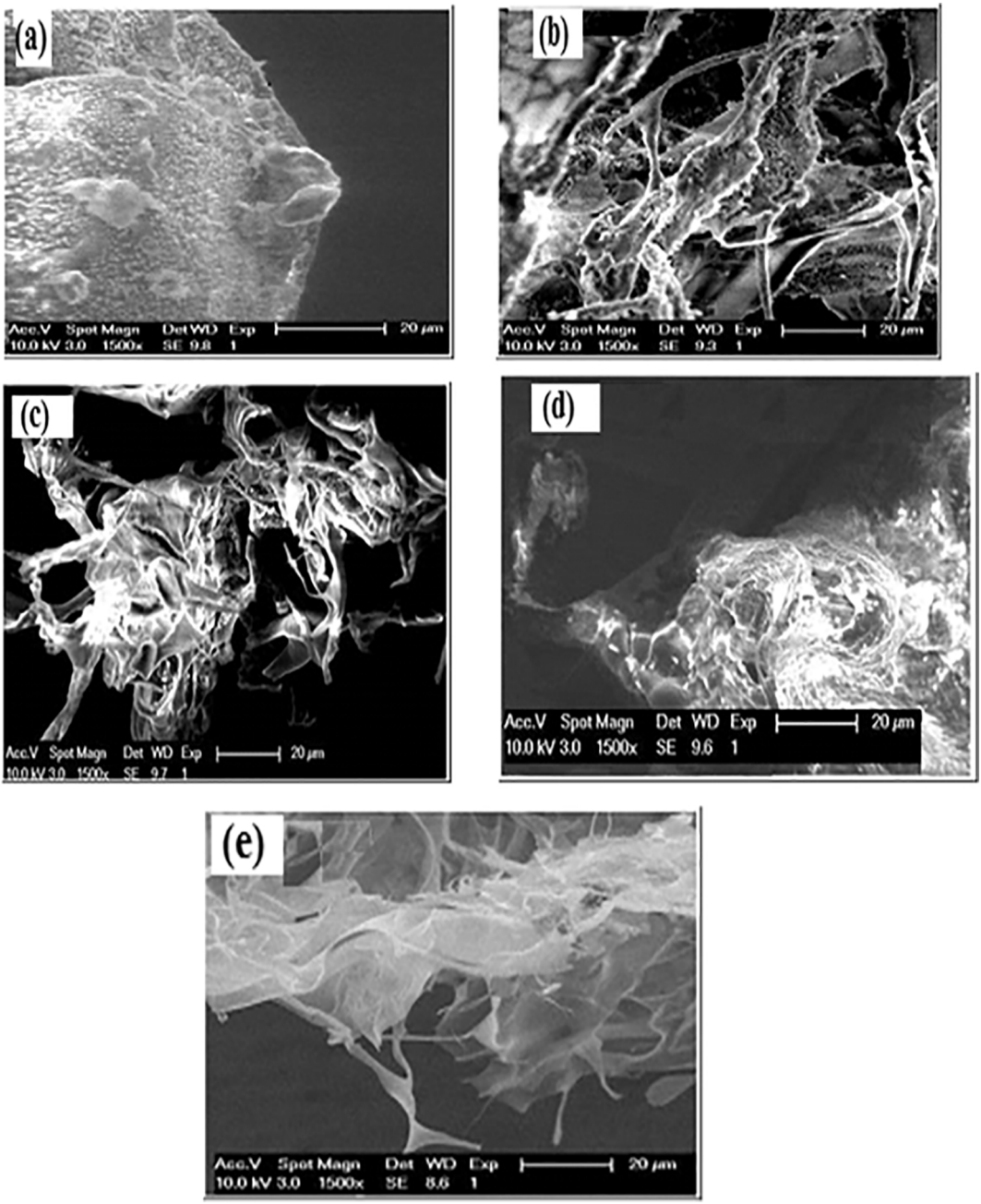
(a)
Acc.V Spot Magn Det WD Exp 20 µm
10.0 kV 3.0 1500x SE 9.8 1
(b)
Acc.V Spot Magn Det WD Exp 20 µm
10.0 kV 3.0 1500x SE 9.3 1
(c)
Acc.V Spot Magn Det WD Exp 20 µm
10.0 kV 3.0 1500x SE 9.7 1
(d)
Acc.V Spot Magn Det WD Exp 20 µm
10.0 kV 3.0 1500x SE 9.6 1
(e)
Acc.V Spot Magn Det WD Exp 20 µm
10.0 kV 3.0 1500x SE 8.6 1

Figure 3

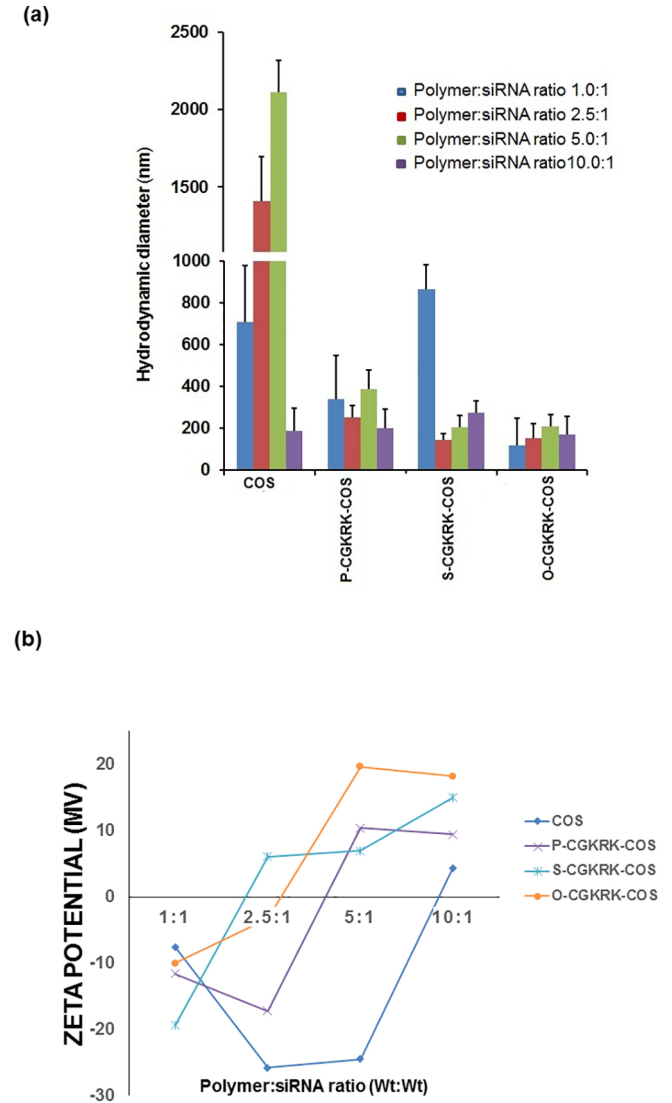
(a)
Hydrodynamic diameter (nm)
2500
2000
1500
1000
800
600
400
200
0
Polymer:siRNA ratio 1.0:1
Polymer:siRNA ratio 2.5:1
Polymer:siRNA ratio 5.0:1
Polymer:siRNA ratio10.0:1
COS
P-CGKRK-COS
S-CGKRK-COS
O-CGKRK-COS
(b)
ZETA POTENTIAL (MV)
20
10
0
-10
-20
-30
1:1
2.5:1
5:1
10:1
Polymer:siRNA ratio (Wt:Wt)
COS
P-CGKRK-COS
S-CGKRK-COS
O-CGKRK-COS

Figure 4

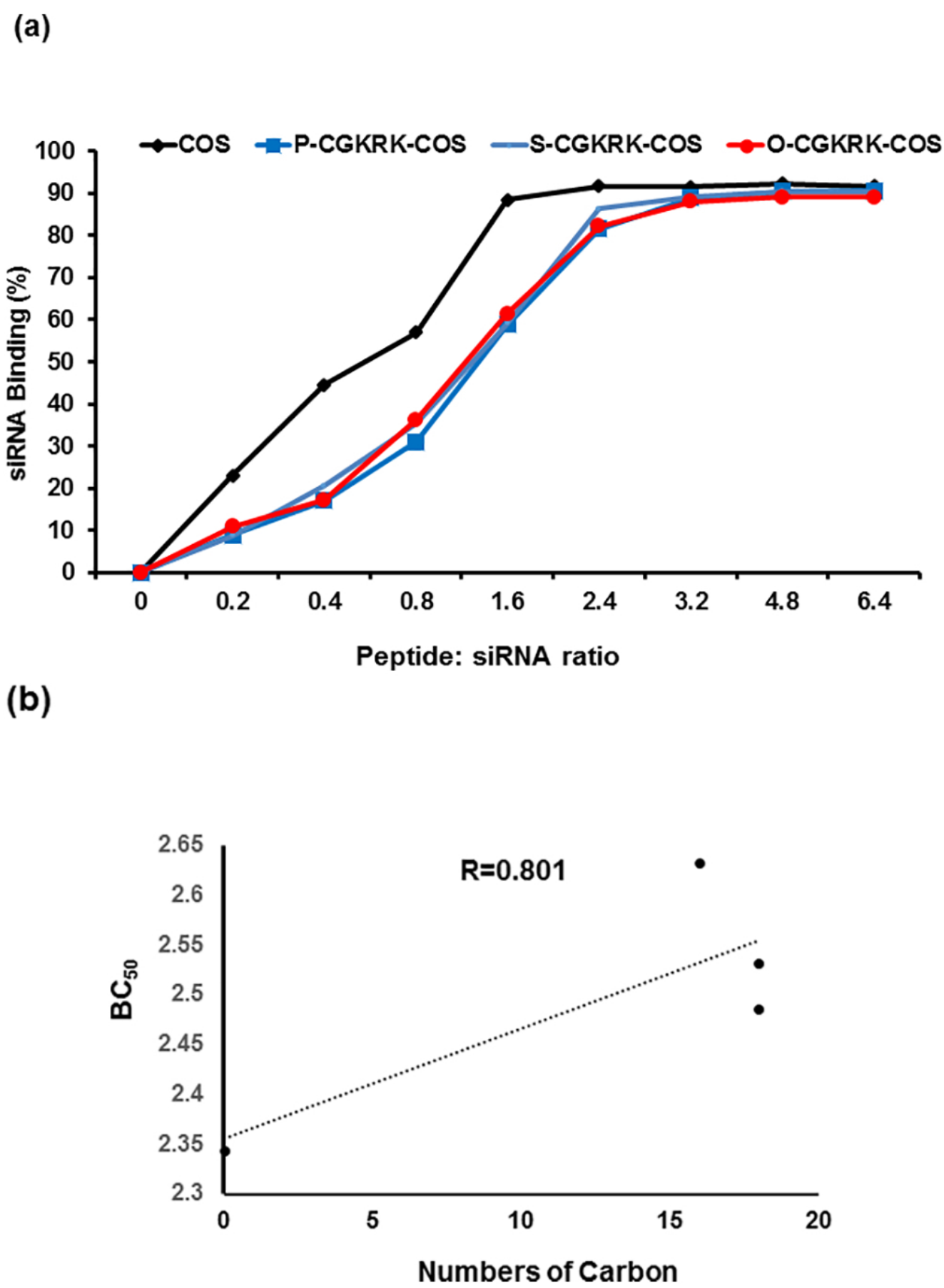
(a)
COS
P-CGKRK-COS
S-CGKRK-COS
O-CGKRK-COS
siRNA Binding (%)
100
90
80
70
60
50
40
30
20
10
0
0
0.2
0.4
0.8
1.6
2.4
3.2
4.8
6.4
Peptide: siRNA ratio
(b)
R=0.801
BC50
2.65
2.6
2.55
2.5
2.45
2.4
2.35
2.3
0
5
10
15
20
Numbers of Carbon

Figure 5

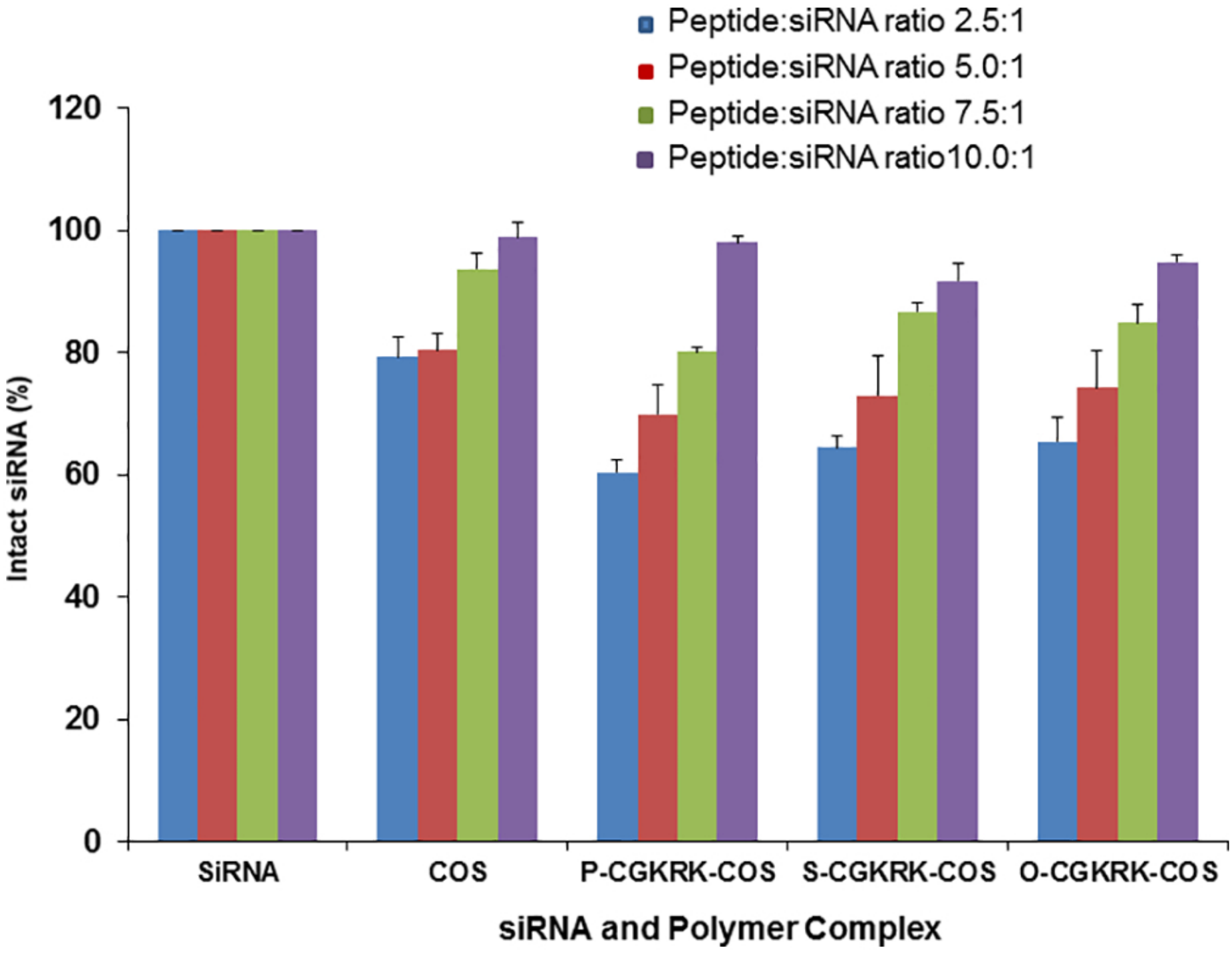
Peptide:siRNA ratio 2.5:1
Peptide:siRNA ratio 5.0:1
Peptide:siRNA ratio 7.5:1
Peptide:siRNA ratio10.0:1
120
100
80
60
40
20
0
Intact siRNA (%)
SiRNA
COS
P-CGKRK-COS
S-CGKRK-COS
O-CGKRK-COS
siRNA and Polymer Complex

Figure 6

(a)

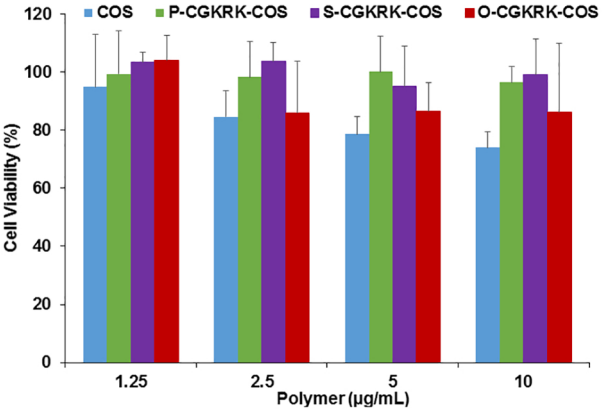
COS
P-CGKRK-COS
S-CGKRK-COS
O-CGKRK-COS
Cell Viability (%)
120
100
80
60
40
20
0
1.25
2.5
5
10
Polymer (μg/mL)

(b)

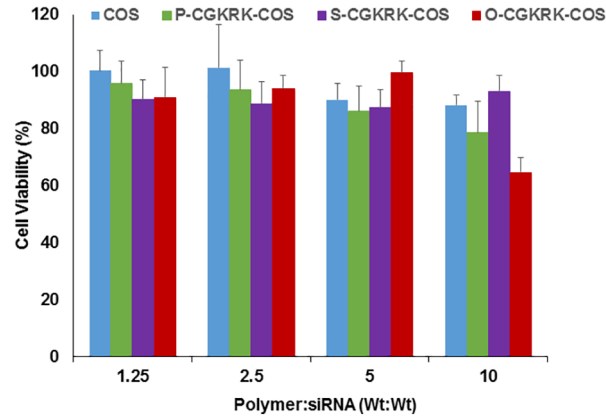
COS
P-CGKRK-COS
S-CGKRK-COS
O-CGKRK-COS
Cell Viability (%)
120
100
80
60
40
20
0
1.25
2.5
5
10
Polymer:siRNA (Wt:Wt)

Figure 7